Molecular Vision 2006; 12:867-78 <http://www.molvis.org/molvis/v12/a98/>
Received 8 February 2006 | Accepted 12 June 2006 | Published 7 August 2006

Characterization of cytokine responses to retinal detachment in rats

Toru Nakazawa,[1] Akihisa Matsubara,[1] Kousuke Noda,[1] Toshio Hisatomi,[1] Haicheng She,[1] Dimitra Skondra,[1] Shinsuke Miyahara,[1] Lucia Sobrin,[1] Kennard L. Thomas,[1] Dong F. Chen,[2] Cynthia L. Grosskreutz,[3] Ali Hafezi-Moghadam,[1] Joan W. Miller[1]

[1]Angiogenesis Laboratory, Massachusetts Eye and Ear Infirmary, Department of Ophthalmology, [2]Schepens Eye Research Institute, Department of Ophthalmology, Program in Neuroscience, [3]Howe Laboratory of Ophthalmology, Massachusetts Eye and Ear Infirmary, Department of Ophthalmology, Harvard Medical School, Boston, MA

Purpose: Photoreceptor apoptosis is associated with retinal detachment (RD) induced photoreceptor degeneration. Previously, we demonstrated the importance of caspase activation for RD-induced photoreceptor death in a rat model of RD. However, extracellular signals that precede the activation of caspases and photoreceptor degeneration remain unclear. The aim of this study is to characterize the molecular and cellular responses that occur after RD. The expression of cytokines, chemokines, and growth factors were examined in a rat model of RD.

Methods: RD was induced in adult rats by subretinal injection of sodium hyaluronate. Retinal tissues were collected at various times (1, 3, 6, 24, and 72 h) after the induction of detachment. To screen for expressional changes in response to RD, major candidates for cytokines, chemokines, and growth factors were broadly examined by quantitative real time polymerase chain reaction (QPCR). To identify the cellular sources of the expressed genes, cells from various layers of the retina were obtained using laser capture microdissection (LCM), and their mRNAs were isolated. Protein expression was quantified by immunohistochemistry and Enzyme Linked-Immuno-Sorbent Assay (ELISA). To assess the potential of early response genes after RD to induce photoreceptor degeneration, exogenous recombinant proteins were subretinally injected and the photoreceptor cell death was assessed using a TdT-dUTP terminal nick-end labeling (TUNEL) assay at 24 h after RD.

Results: At 72 h after RD a significant increase in mRNA levels for tumor necrosis factor α (TNF-α), interleukin-1β (IL-1β), monocyte chemotactic protein-1 (MCP-1), and basic fibroblast growth factor (bFGF) were detected in the neural retina. LCM revealed increased expression of mRNA for bFGF and MCP-1 in all retinal layers, though bFGF was especially evident in the outer nuclear layer (ONL) and MCP-1 in the inner nuclear layer (INL). TNF-α was increased in the ONL and the INL, and IL-1β was increased in the ganglion cell layer. Time course experiments showed that TNF-α, IL-1β and MCP-1 increased within 1 h after RD, while bFGF was increased by 24 h. Increased protein expression for TNF-α, IL-1β, and MCP-1 was demonstrated by ELISA at 6 h after RD. Immunohistochemistry showed TNF-α and bFGF expression in the whole retina, with IL-1β specifically expressed in astrocytes and MCP-1 in Müller cells. Subretinal administration of MCP-1 significantly increased TUNEL-positive cells in the ONL 24 h after RD, while injection of vehicle control, TNF-α, or IL-1β showed no effect.

Conclusions: Retinal glial cells, including astrocytes and Müller cells, are a major source of cytokine induction after RD. The increased expression and release of MCP-1 may be an important cause of photoreceptor degeneration associated with RD. This study helps to understand the mechanisms of RD-induced photoreceptor degeneration. Our results may provide new therapeutic targets to prevent photoreceptor degeneration following RD.

Photoreceptor apoptosis is associated with human retinal detachment (RD) induced photoreceptor degeneration [1-4]. Previously, we demonstrated the importance of caspase activation in RD-induced photoreceptor death in a rat model of RD [5,6]. However, the upstream extracellular signals that lead to caspase activation and ultimately to photoreceptor degeneration after RD remain unclear.

Cytokines, chemokines, and growth factors are extracellular proteins that can regulate caspase activity and apoptotsis of cells in response to injury. For instance, the cytokine TNF-α induces a signal transduction cascade that activates caspase 8, which triggers the cleavage of caspase 3 and leads to apoptosis [7]. In contrast, growth factors, such as bFGF and neurotrophins, stimulate Akt, which suppresses the activation of caspase 9 and subsequent downstream events to support neuronal survival [8]. Thus, better understanding of the roles of cytokines and growth factors in RD will provide further insight into the mechanisms leading to photoreceptor cell death.

Cytokines also play a pivotal role in proliferative changes of the retina associated with RD, including Müller cell hypertrophy [9-11], neovascularization, and neoplasia, as well as proliferative vitreoretinopathy (PVR) [12,13]. These proliferative changes are often serious complications and are associated with a poor prognosis even after surgery [14,15]. Vitreous samples from patients with RD contain significantly higher levels of TNF-α [16,17], IL-1β [14,16], MCP-1 [18-20], and bFGF [14,15,21,22] compared to samples from patients with a macular hole or idiopathic premacular fibrosis. Despite the

Correspondence to: Joan W. Miller, Angiogenesis Laboratory, Massachusetts Eye and Ear Infirmary, Department of Ophthalmology, Harvard Medical School, 325 Cambridge street, Boston, MA, 02114; Phone: (617) 573-6425; FAX: (617) 573-3078; email: Joan_Miller@meei.harvard.edu

association of cytokines and growth factors with PVR and photoreceptor death, the mechanisms that induce cytokine release and their roles in RD are largely unexplored.

In this study, in order to characterize cytokine, chemokine, and growth factor responses to RD, we screened for the changes in gene expression in the neural retina following RD using quantitative real-time PCR (QPCR). We also characterized the changes of TNF-α, IL-1β, MCP-1, and bFGF following RD in the various retinal layers using Laser Capture Microdissection (LCM), QPCR, Enzyme Linked-Immuno-Sorbent Assay (ELISA) and immunohistochemistry.

METHODS

Animals: All procedures concerning animals were performed in accordance with the statement of the Association for Research in Vision and Ophthalmology and the approval of the Animal Care Committee of the Massachusetts Eye and Ear Infirmary. Adult male Brown Norway rats (200-300 g, Charles River, Boston, MA) were housed in covered cages, fed with standard rodent diet ad libitum, and kept on a 12 h light/dark cycle.

Surgical procedure of RD: The rat RD was performed as previously described [5]. Adult male rats were anesthetized with a mixture (1:1) of ketamine (100 mg/ml) and xylazine (20 mg/ml; both from Phoenix Pharmaceutical, St. Joseph, MO). A total of 84 rats were used for this study. Pupils were dilated with a topically applied mixture of phenylephrine (5.0%) and tropicamide (0.8%). A sclerotomy was performed approximately 2 mm posterior to the limbus using a 30-gauge needle, while being cautious not to damage the lens during the procedure. A Glaser subretinal injector (20-gauge shaft with a 32-gauge tip, BD Biosciences) connected to a syringe filled with sodium hyaluronate (Healon, Pharmacia and Upjohn Co., Kalamazoo, MI) was then introduced into the vitreous cavity. Retinotomy was performed in the peripheral retina with the tip of the subretinal injector, and the sodium hyaluronate was slowly injected into the subretinal space, causing detachment of one half of the retina. Subretinal administration of 5 μl PBS (0.1 M phosphate buffer [pH, 7.4] -0.15 M NaCl), rat recombinant TNF-α (Peprotech, Rocky Hill, NJ, 0.1 μg/μl), rat recombinant IL-1β (Peprotech, 0.1 μg/μl) or rat recombinant MCP-1 (Peprotech, 0.1 μg/μl) was additionally performed following RD, using a Hamilton syringe equipped with a 32-gauge needle and introducing the tip of the needle through the sclerotomy and retinal hole into the subretinal space and then injecting 5 μl of solution over 3 min. RDs were induced only in the right eye of each animal, with the left eye serving as a control. At specified times after RD, rats were sacrificed with an overdose of sodium pentobarbital, and the eyes were enucleated.

RNA extraction and reverse transcription (RT)-PCR: Total RNA extraction and RT-PCR was performed as previously reported with minor modification [23]. Briefly, total RNA was extracted using the RNA Purification System (Invitrogen, Carlsbad, CA). Each retina was homogenized with 600 μl of RNA lysis buffer and mixed with an equivalent volume of 70% ethanol. The mixture was applied to the RNA spin cartridge, centrifuged at 12,000 g for 15 s at 25 °C, and washed with wash buffers I and II. The total RNA was eluted with 30 μl of RNase-free water. To minimize potential contamination of genomic DNA, RNA samples were incubated with DNase I (Invitrogen) for 15 min at room temperature. The total RNA concentration was measured using an UV spectrophotometer (UV-1201, Shimadzu corp., Kyoto, Japan). Three μg of total RNA was subjected to RT using the SuperScript III First-Strand Synthesis System (Invitrogen). First strand cDNAs were amplified using a real-time PCR thermal cycler (ABI7700, Applied Biosystems, Foster City, CA). QPCR was performed with Sybergreen PCR core kit (Applied Biosystems) as previously reported [23]. Genes were selected that have been widely reported to be involved in patients with RD, and/or respond to neural injury in the experimental animal model. Table 1 lists the PCR primers used in this study. PCR products were confirmed by agarose gel electrophoresis. For relative comparison of each gene, we analyzed the C_t value of the real-time PCR data with $\Delta\Delta C_t$ method [24] according to the manufacturer's instructions (Applied Biosystems). To normalize the amount of sample cDNA added to each reaction, the C_t value of the endogenous control (18rRNA) was subtracted from the C_t value of each target gene.

Laser capture microdissection (LCM): LCM (Arcturus PixCell IIe Laser Capture Microdissection System, Arcturus, Mountain View, CA) is a recently developed technology that allows the capture of specific cells in a histological section using laser irradiation [25,26]. Using this technique, we are able to harvest different retinal cells by collecting samples from individual retinal layers (Ganglion cell layer: retinal ganglion cells, displaced amacrine cells, and astrocytes, Inner nuclear layer: amacrine cells, bipolar cells, horizontal cells, and Müller glial cells, Outer nuclear layer: photoreceptor cells, and Retinal pigment epithelium layer: pigment epithelial cells). To investigate the cellular origin of the gene expression, LCM was performed as previously described [26]. Briefly, 72 h after RD, the eyes were enucleated and embedded in Tissue-Tek OCT compound (Sakura Finetechnical Co., Ltd., Tokyo, Japan). Transverse retinal sections (12 μm) that included the optic nerve were cut with a cryostat (Micron, Germany) and mounted on Superfrost Plus glass slides (Fisherbrand, Pittsburgh, PA). Tissue sections were rehydrated by 75% ethanol, twice with DEPC water, followed by dehydration with 75%, 95%, and 100% ethanol for one min each, and Xylene for 5 min. LCM for cells in the ganglion cell layer (GCL) or retinal pigment epithelium layer (RPE) was carried out at 70 mW for 0.75 s and a spot size of 7.5 μm. LCM for cells of the inner nuclear layer (INL) and outer nuclear layer (ONL) was carried out at 90 mW for 1.2 s and a spot size of 15 μm. LCM was performed in 16 retinal sections, on cells in areas of the detached retina or those in the corresponding region of the left (undetached) eye. RNA was extracted with PicoPure™ RNA Isolation Kit (Arcturus, catalog number KIT0202) followed by DNase treatment (Qiagen, catalog number 79254). Total RNA was eluted in 30 μl of Elution Buffer, and 24 μl of the total RNA was used for QPCR.

ELISA: The tissue complex containing the posterior lens

capsule, the vitreous, and the neural retina was collected at 6 and 72 h after RD. Proteins of each retina were extracted in 100 µl of PBS containing the protease inhibitor cocktail (Complete, Roche Diagnostics) and sonicated at 10 watts (BRANSON SONIFIER 250, Danbury, CT) for 5 s on ice. The supernatant was collected following centrifugation at 14,000 g for 10 min at 4 °C (Micromax RF, IEC, Needham heights, MA), and the total protein concentration was measured using the DC protein assay kit (Bio-Rad, Hercules, CA). Two hundred µg of total protein was used for ELISA (Biosource, Camarillo, CA), performed according to the manufacturer's guidelines. The absorbance at 450 nm wavelength was measured using a 96 well plate by spectrophotometry (Spectramax 190, Molecular decevice, Sunnyvale CA).

Immunohistochemistry: Immunohistochemistry was performed as previously reported [27-30]. Briefly, after perfusion of the animals with 30 ml PBS and then 30 ml of 4% paraformaldehyde (PFA), the eyes were enucleated and post-

Table 1. Primer set for real-time PCR

Gene name	Sense primer	Antisense primer
18rRNA	CAGTGAAACTGCGAATGGCTCATT	CCCGTCGGCATGTATTAGCTCTAGA
FGF2	TCTTCCTGCGCATCCATCCAGA	CAGTGCCACATACCAACTGGAG
BDNF	CTTGGACAGAGCCAGCGGATTTGT	CCGTGGACGTTTGCTTCTTTCATG
NT-3	TCTGCCACGATCTTACAGGTGAACA	CGCCTGGATCAACTTGATAATGAGG
NT-4	TACCCTGGCAAGAGAGACGAGGAA	CCACCGTGCATGGTTTATGATACG
GDNF	TGCCCTTCGCGCTGACCAGTGACA	TTCGAGGAAGTGCCGCCGCTTGTT
IGF-1	TTCAGTTCGTGTGTGGACCAAGG	GCTTCAGCGGAGCACAGTACATCT
HGF	AGATGAGTGTGCCAACAGGTGCAT	AGGTCAAATTCATGGCCAAACCC
PDGFA	CACTGTTAAGCATGTGCCGGAGAA	CCAGATCAAGAAGTTGGCCGATGT
PDGFB	CTTGAACATGACCCGAGCACATTCT	ATCGATGAGGTTCCGCGAGATCT
TNF-α	CCCAGACCCTCACACTCAGATCAT	GCAGCCTTGTCCCTTGAAGAGAA
IL-1β	TCAGGAAGGCAGTGTCACTCATTG	ACACACTAGCAGGTCGTCATCATC
TGF-β	AATGGCTCTCCTTCGACGTGACA	CCTCCAGCTCTTGGCTCTTATTTGG
CNTF	GCCGTTCTATCTGGCTAGCAAGGA	GCCTCAGTCATCTCACTCCAACGA
MCP-1	ATGCAGGTCTCTGTCACGCTTCTG	GACACCTGCTGCTGGTGATTCTCTT
VEGF	TCTTCCAGGAGTACCCCGATGAGA	GGTTTGATCCGCATGATCTGCAT
Angiopoietin-1	GCCCAGATACAACAGAATGCGGTT	CTCCAGCAGTTGGATTTCAAGACG
Angiopoietin-2	CTCGGAAACTGACTGATGTGGAAGC	TGTCCTCCATGTCCAGCACTTTCTT
CTGF	ACCCAACTATGATGCGAGCCAACT	AATTTTAGGCGTCCGGATGCACT
PEDF	GCTGTTTCCAACTTCGGCTACGAT	AGAGAGCCCGGTGAATGACAGACT

Nineteen primer sets for cytokines, chemokines, growth factors, and one internal control (18rRNA) were used in this study.

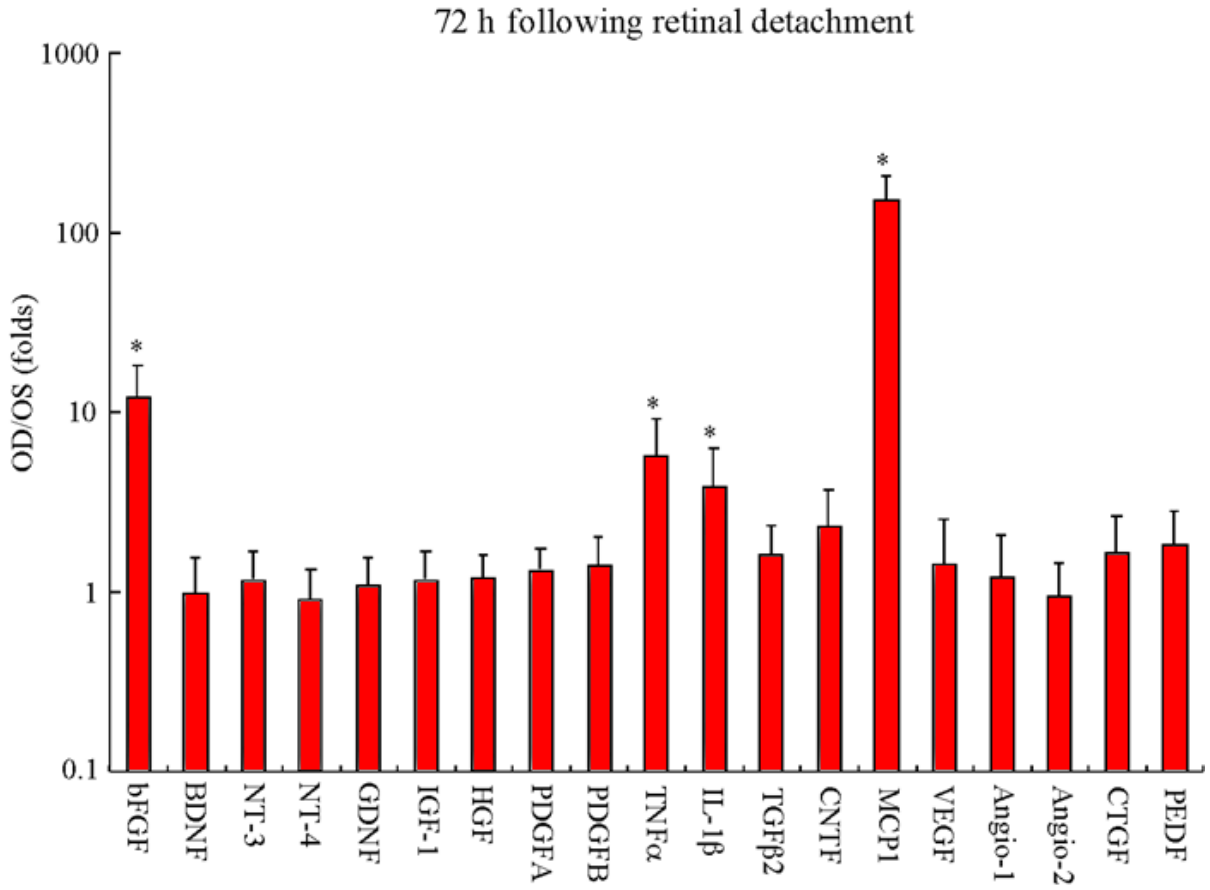

Figure 1. Changes in growth factor and cytokine expression in neural retina after retinal detachment. Quantitative analysis (these data are from 6 different eyes) of the induction of growth factor and cytokine mRNAs by QPCR at 72 h after RD. Y-axis represents the ratio of mRNA expression in the experimentally detached retina of the right eye (OD) to that of the control left eye (OS). bFGF represents basic fibroblast growth factor; BDNF represents brain represents derived neurotrophic factor; NT-3 represents neurotrophin-3; NT-4 represents neurotrophin-4; GDNF represents glial cell line-derived neurotrophic factor; IGF-1 represents insulin-like growth factor-1; HGF represents hepatocyte growth factor; PDGFA and PDGFB represent platelet-derived growth factors A and B; TNF-α represents tumor necrosis factor-α; IL-1β represents interleukin-1β; TGF-β2 represents transforming growth factor β 2; CNTF represents ciliary neurotrophic factor; MCP-1 represents monocyte chamoattractant protein-1; VEGF represents vascular endothelial growth factor; Angio-1 and Angio-2 represents angiopoietin-1 and angiopoietin-2; CTGF represents connective tissue growth factor; PEDF represents pigment epithelium-derived factor. Asterisks (*) indicate significant difference ($p<0.05$) compared to control eyes.

fixed in PFA (4% at 4 °C overnight). Eyes were cut to be eye cups and cryoprotected with 20% sucrose in PBS. Retinal specimens were frozen in OCT, and 10 µm retinal sections that included the optic nerve were cut on a cryostat. Sections were mounted onto Superfrost glass slides, preblocked with PBS containing 10% goat serum, 0.5% gelatin, 3% BSA, and 0.2% Tween20, followed by incubation with polyclonal rabbit anti-bFGF (Santa Cruz Biotech. Inc., Santa Cruz, CA, 1:200), TNF-α (Pierce Biotechnology, Inc., Rockford, IL, 1:200), IL-1β (Pierce Biotechnology, Inc., 1:200) or MCP-1 (Peprotec, Rocky Hill, NJ, 1:200). For some sections, mouse monoclonal antibody against glial fibrillary acidic protein (GFAP, Sigma, 1:400), a marker for astrocytes, or glutamine synthetase (BD Biosciences, San Diego, CA, 1:200)-a marker of Müller cells-were used to label retinal glial cells. The reaction buffer without the primary antibody was used as negative control. Sections were then incubated with a fluorescent secondary antibody, goat anti-mouse immunoglobulin G (IgG) or anti-rabbit IgG conjugated to either Alexa Fluor 546 or Alexa Fluor 488 (Molecular Probes). Sections were mounted with Vectashield mounting media and stained with propidium iodide or DAPI (Vector Laboratories, Burlingame, CA). Photomicrographs of the retinal sections were taken at a distance of 2 mm from the center of the optic nerve head using fluorescent microscopy (DMRXA, Leica) and OpenLab software version 2.2.5 (Improvision Inc., Lexington, MA).

TUNEL: Eyes were harvested 24 h or 72 h after RD, fixed overnight with 4% PFA, and cryoprotected with 20% sucrose. TUNEL was performed as previously described [29] using the ApopTag Fluorescein In Situ Apoptosis detection kit (S7110, Chemicon International, Inc., Temecula, CA). The center of the detached retina was photographed, and the number of TUNEL-positive cells in the outer nuclear layer (ONL) was counted in a masked fashion.

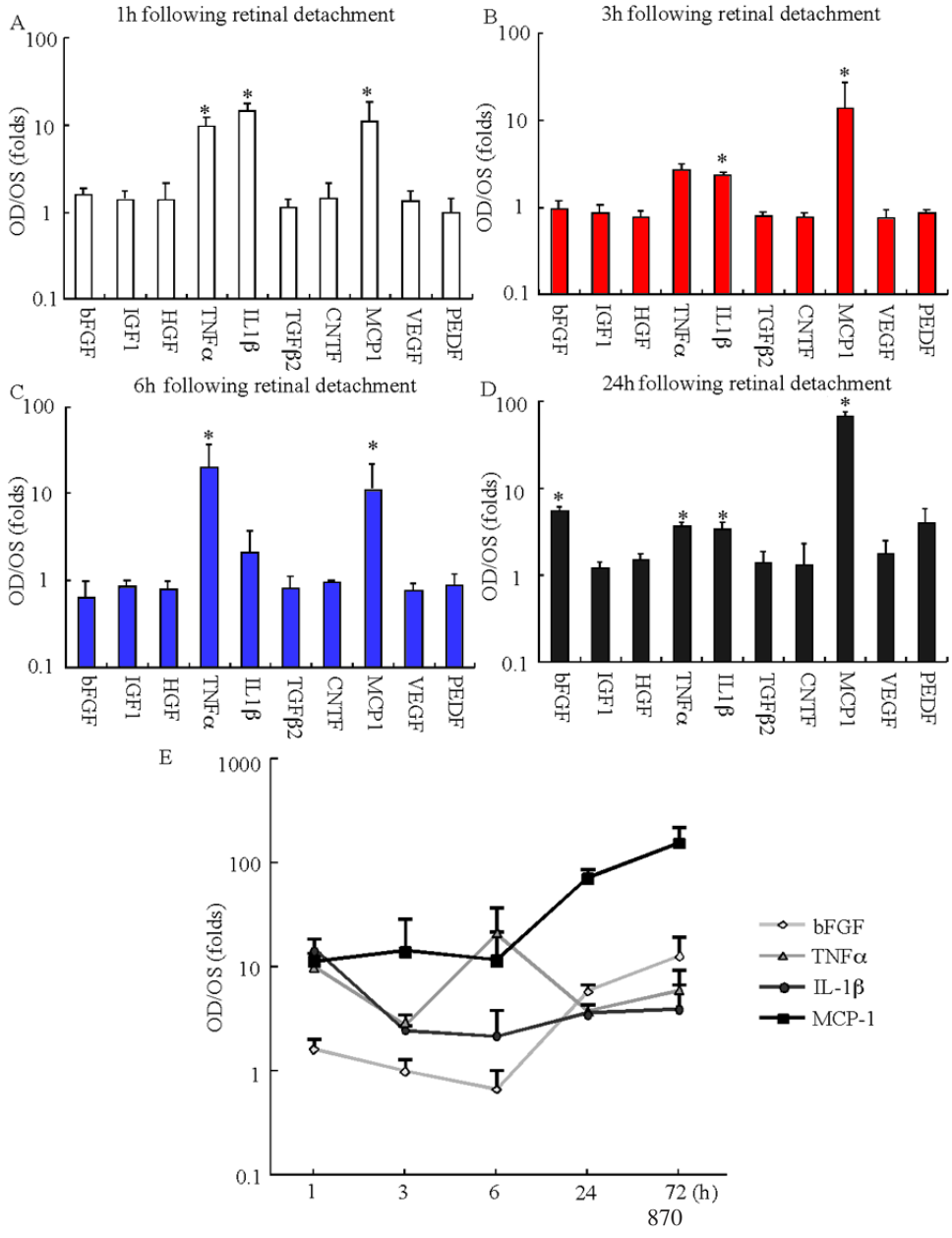

Figure 2. Time course study of cytokine induction after retinal detachment. **A**-**D**: Quantification by QPCR of RD-induced expression of various cytokines at 1 (**A**), 3 (**B**), 6 (**C**), and 24 h (**D**) after RD (n=6). Note that the mRNA levels of TNF-α, IL-1β, and MCP-1 were significantly increased at 1 h after RD, while the induction of bFGF was not detected until 24 h. **E**: Summary of time course studies for the induction of bFGF, TNF-α, IL-1β, and MCP-1 after RD. Asterisks (*) indicate significant difference ($p<0.05$) compared to control eyes.

Statistical analysis: Statistical analysis of the RT-PCR and ELISA data were performed using the unpaired t-test. The data from the TUNEL assay was analyzed with the Scheff post hoc test using the StatView software (version 4.11J, Abacus concepts Inc., Berkeley, CA) on a Macintosh computer. $p<0.05$ were considered statistically significant and were highlighted in the figures with an asterisk. All values are expressed as the mean±standard deviation (SD) unless noted otherwise.

RESULTS

RD-induced changes in cytokine, chemokine, and growth factor levels: To screen for cytokine, chemokine, and growth factor genes associated with RD, we quantified in rats expression of 19 different genes with QPCR at 72 h after RD, when photoreceptor cell loss reaches its peak [5,31]. In comparison with the control eye, the expression of four genes, bFGF (12.0 fold), TNF-α (5.7 fold), IL-1β (3.8 fold) and MCP-1 (149.3 fold), was significantly upregulated in the detached retina, while the expression of other cytokines and growth factors examined did not change significantly (Figure 1).

To determine the time course of the cytokine response to RD, retinal tissues were harvested at 1, 3, 6, 24, and 72 h after the induction of RD, and mRNA levels of various cytokines and growth factors were analyzed. Except for bFGF, for which

Table 2. Quantification of TNF-a, IL-1b, and MCP-1 expression by ELISA

GOI	6 h RD+	6 h RD-	p value	72 h RD+	72 h RD-	p value
TNFα	95.4±6.0	46.1±1.2	0.00348*	50.7±3.8	40.9±1.6	0.0418*
IL-1β	103.4±9.6	51.9±0.6	0.01368*	55.0±1.9	44.4±1.1	0.0009*
MCP-1	88.2±6.6	9.8±0.2	0.00119*	94.1±2.7	9.2±0.6	0.0001*

Retinal samples were collected at 6 and 72 h after RD, respectively (6/group). The data represent cytokine level of ELISA obtained in the experimentally detached retina (RD+) and that of the control eye (RD-). Data represents mean±SEM. GOI represents gene of interest.

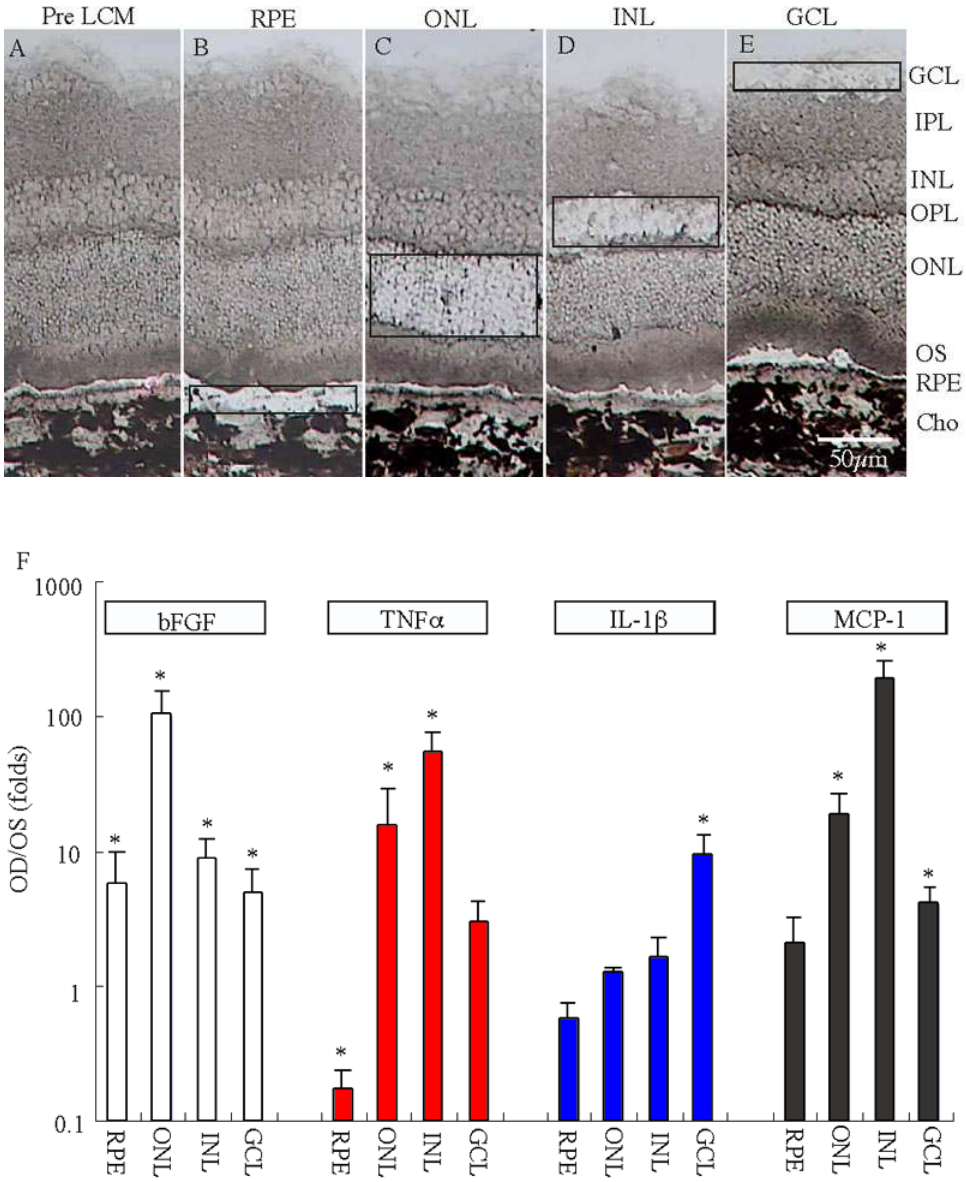

Figure 3. Expressional changes of cytokines in individual retinal layers: laser capture microdissection. **A**-**E**: Representative photomicrographs of retinal sections taken before (**A**) and after LCM (**B**-**E**). Black rectangle indicates the retinal layer where LCM was performed. **F**: Quantitative analysis of RNA samples obtained by LCM with QPCR to determine levels of bFGF, TNF-α, IL-1β, and MCP-1 mRNAs in different layers of the retina (n=6). The ganglion cell layer (GCL), inner plexiform layer (IPL), inner nuclear layer (INL), outer plexiform layer (OPL), outer nuclear layer (ONL), outer segment (OS), retinal pigment epithelium (RPE), and choroid (Cho) are identified. Asterisks (*) indicate significant difference ($p<0.05$) compared to control eyes.

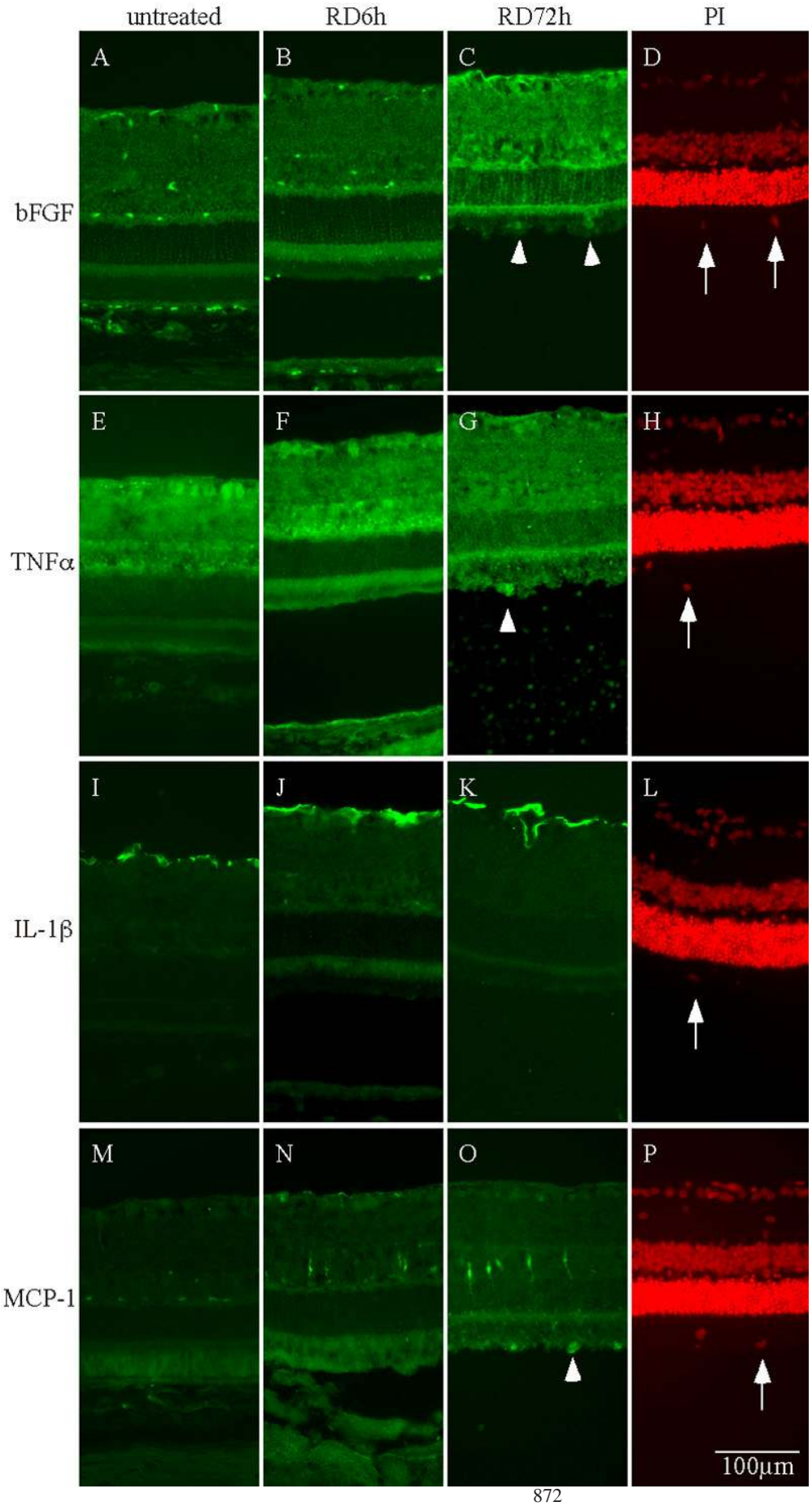

Figure 4. Immunohistochemical analysis of cytokines after RD. Representative photomicrographs of retinal sections labeled with primary antibodies against bFGF (**A**-**D**), TNF-α (**E**-**H**), IL-1β (**I**-**L**), and MCP-1 (**M**-**P**) or nuclear staining dye propidium iodide (PI: **D**,**H**,**L**,**P**). The retinal sections were derived from the control eye (**A**,**E**,**I**,**M**) or those at 6 (RD 6 h; **B**,**F**,**J**,**N**) or 72 h after RD (RD 72 h; **C**,**G**,**K**,**O**; n=4 each). Arrows point to monocytes, and arrowheads indicate the positive immunoreactivity of bFGF (C), TNF-α (**G**), or MCP-1 (**O**). Note that immunoreactivity of bFGF appeared in retinal sections at 72 h after RD; whereas, the upregulation of TNF-α, IL-1β, and MCP-1 immunoreactivity started by 6 h.

an increased expression was not detected until 24 h after RD (Figure 2D,E), the mRNA levels of TNF-α, IL-1β, and MCP-1 were significantly upregulated as early as 1 h after RD (Figure 2A,E). Expression of MCP-1 continued to increase after 24 h and reached its highest level at 72 h after RD. Expression of IL-1β, however, was highest at 1 h after RD, declined thereafter and then remained constant for up to 72 h after RD, while TNF-α gene expression revealed 2 peaks, at 1 and 6 h after RD.

To further investigate the expression of these cytokines at the protein level, we performed ELISA with vitreous and retinas collected at 6 and 72 h after RD. At these times, total protein levels did not vary between control and RD groups. However, TNF-α (2.2 fold), IL-1β (2.0 fold), and MCP-1 (9.0 fold) protein levels were significantly elevated in the detached retinas at 6 h after RD in comparison with the control retinas (Table 2). At 72 h after RD, MCP-1 protein expression was still significantly higher by 10.2 fold compared to undetached retina. While the TNF-α (1.2 fold) and IL-1β (1.2 fold) protein expression was decreased but still significantly higher compared to undetached control retina (Table 2). These results suggest that TNF-α, IL-1β, and MCP-1 mRNA and protein expression is induced in response to RD and that these factors may play a role in RD-associated photoreceptor cell damage.

Cellular origin of cytokine responses: We used the established method of LCM to identify the cellular origin of the cytokines after RD. At 72 h after RD, cells located in the various retinal layers (GCL, INL, ONL, and RPE) were collected by LCM. The mRNA levels of TNF-α, IL-1β, MCP-1, and

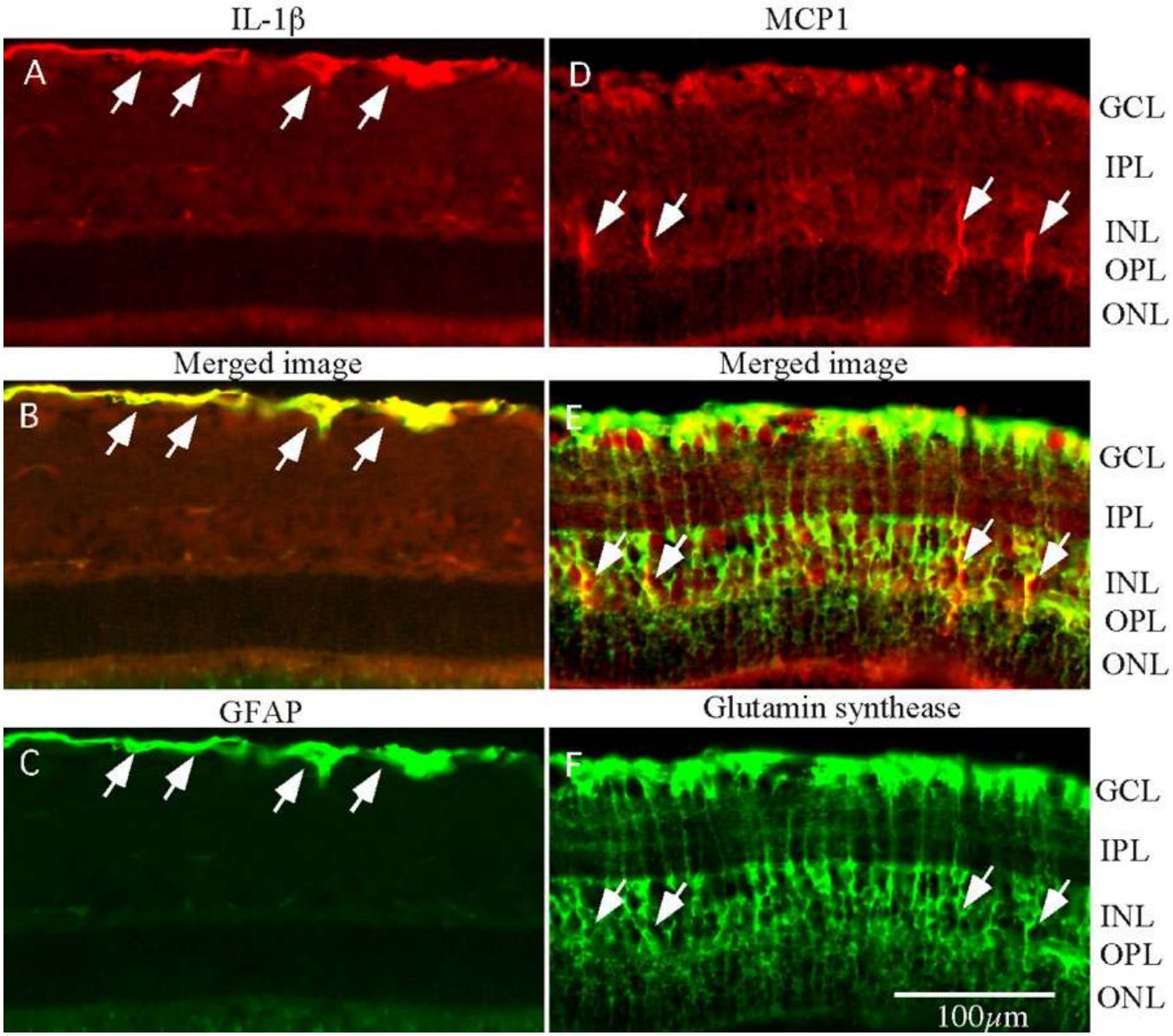

Figure 5. Cellular source of cytokines after RD. Co-localization of IL-1β (**A**-**C**) and MCP-1 (**D**-**F**) immunoreactivity (red) with markers for astrocytes-GFAP (**A**-**C**), or Müller glial cells-glutamine synthetase (**D**-**F**; green). Arrows point to astrocytes in (**A**-**C**) or to Müller glial cells in (**D**-**F**).

bFGF were analyzed using QPCR (Figure 3). A significant increase of TNF-α mRNA was found in the INL and the ONL whereas induction of IL-1β was limited to the GCL. The increase of MCP-1 mRNA was detected in all retinal layers save for the RPE, while the highest expression was detected in the INL. In addition, the mRNA of bFGF was also significantly increased in all retinal layers, with its highest expression in the ONL.

To corroborate the protein distribution of TNF-α, IL-1β, MCP-1, and bFGF, we performed immunohistochemistry at 6 and 72 h after RD. In the normal retina, TNF-α was detected in the GCL and the INL, while the immunoreactivity for bFGF was weakly distributed in the entire retina (Figure 4A,E). IL-1β was detected in the vitreal surface of the GCL (Figure 4I), while MCP-1 was detected at a low level in the GCL and the INL (Figure 4M). Consistent with our mRNA-expression data, an increase in the immunoreactivity of TNF-α, IL-1β, and MCP-1, but not bFGF, was detected in the detached retinas at 6 h after RD (Figure 4). Similar to the results obtained from LCM studies, the increase of TNF-α was located in the INL and ONL (Figure 4F), while the expression of IL-1β was upregulated in the GCL (Figure 4J). Immunoreactivity of MCP-

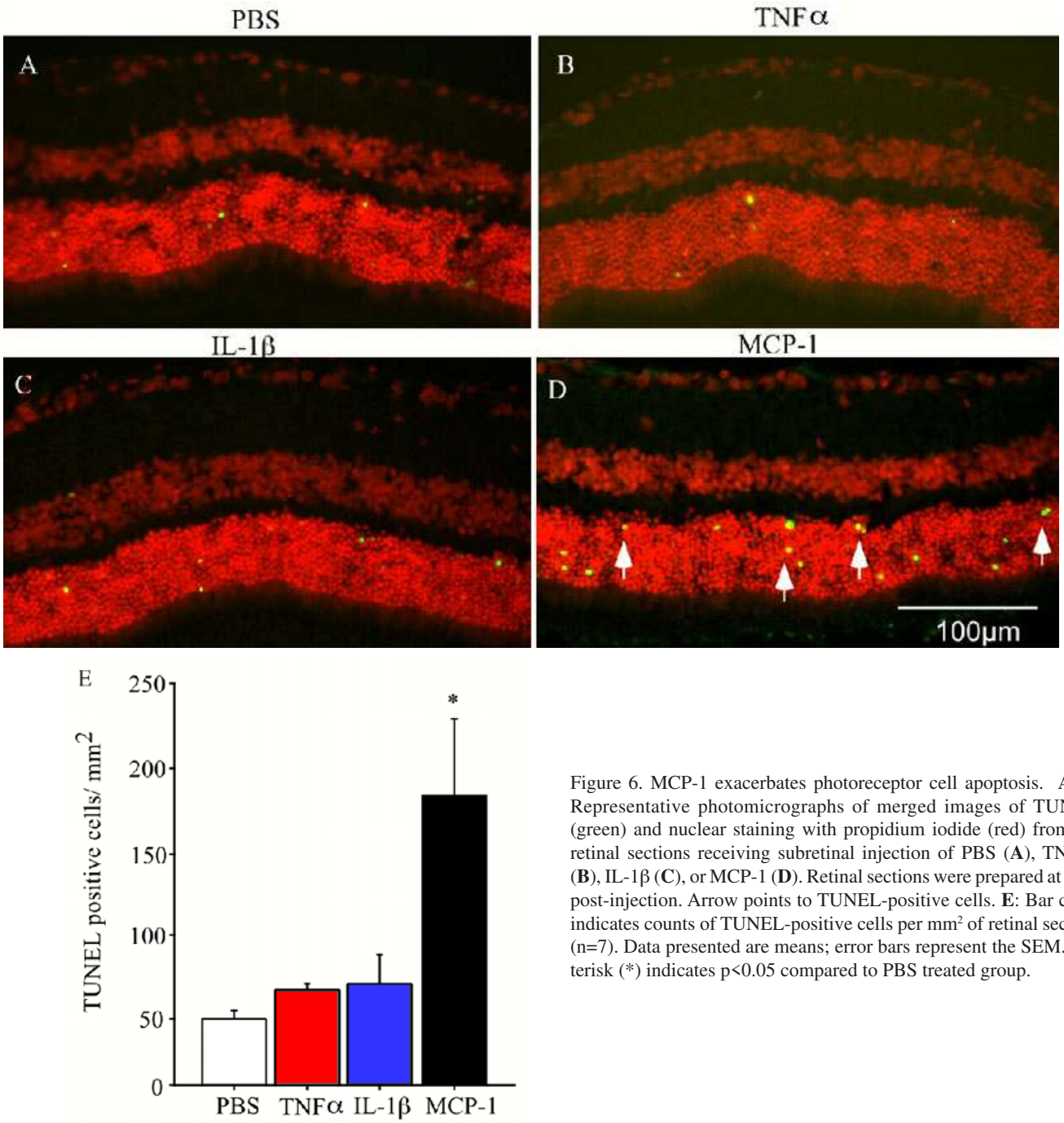

Figure 6. MCP-1 exacerbates photoreceptor cell apoptosis. **A**-**D**: Representative photomicrographs of merged images of TUNEL (green) and nuclear staining with propidium iodide (red) from rat retinal sections receiving subretinal injection of PBS (**A**), TNF-α (**B**), IL-1β (**C**), or MCP-1 (**D**). Retinal sections were prepared at 24 h post-injection. Arrow points to TUNEL-positive cells. **E**: Bar chart indicates counts of TUNEL-positive cells per mm^2 of retinal section (n=7). Data presented are means; error bars represent the SEM. Asterisk (*) indicates $p<0.05$ compared to PBS treated group.

1 was increased primarily in the INL and weaker signal was also detected in GCL at 6 h after RD and continued to increase up to 72 h, with a staining pattern resembling that of Müller glial cells, which have cellular processes spanning the retina (Figure 4N,O). The increased bFGF immunoreactivity was detected in all retinal layers. Consistent with previous reports [31,32], 72 h after RD monocytes are detected in the subretinal space attached to the outer segment of photoreceptors (Figure 4 arrow). These monocytes show immunoreactivity for bFGF, TNF-α, and MCP-1 (Figure 4, arrowhead).

To further identify the cell populations that produce IL-1β or MCP-1, the two factors displaying layer-specific distribution in the retina, we labeled the retinal sections with antibodies against glial fibrillary acidic protein (GFAP) for astrocytes and glutamine synthetase for Müller cells. The labeling of IL-1β was co-localized with the astrocyte marker GFAP (Figure 5A-C), while the immunostaining of MCP-1 was co-localized with that of glutamine synthetase, the Müller cell marker (Figure 5D-F). Our results indicate that retinal glial cells, including astrocytes and Müller cells, are responsible for the upregulation of IL-1β and MCP-1 following RD.

MCP-1 induced photoreceptor apoptosis: To determine whether the three earliest responding cytokines, TNF-α, IL-1β, and MCP-1, play a role in photoreceptor degeneration after RD, we injected these factors subretinally as recombinant protein during RD induction and assessed photoreceptor cell death. Cell death was quantified by TUNEL assay 24 h after RD, since at that time the number of TUNEL-positive cells in the ONL is reported to be small [31]. Consistent with the prior report [31], occasional cell apoptosis was observed in the ONL of the PBS-treated group (n=7; Figure 6A,E). Also, subretinal injection of TNF-α (0.1 μg/μl; n=7) or IL-1β (0.1 μg/μl; n=7) did not increase the number of TUNEL-positive cells in the retina in comparison with the PBS-treated group. In contrast, subretinal administration of MCP-1 (0.1 μg/μl) induced a significant increase of TUNEL-positive cells in the ONL at 24 h post-injection ($p<0.02$), suggesting that this chemokine may have a toxic effect on photoreceptors.

DISCUSSION

Understanding the pathogenesis of RD, which includes photoreceptor cell death, proliferative changes (PVR) and Müller cell hypertrophy (retinal gliosis), is of great clinical importance. To explore the pathogenesis of RD, we screened for the expressional changes of genes including cytokines, chemokines, and growth factors in a rat model of RD. Our study indicates that RD induces upregulation of TNF-α, IL-1β and MCP-1 as early as 1 h after injury. Retinal glial cells (astrocytes and Müller cells) are the primary source of the IL-1β and MCP-1. We also show that MCP-1 has a neurotoxic role in photoreceptor degeneration with RD. To our knowledge, this is the first evidence suggesting an association between MCP-1 and photoreceptor cell death.

Our QPCR data show that mRNA for TNF-α, IL-1β, MCP-1 and bFGF are increased by 72 h after RD. Our findings are in agreement with the reports of increased cytokine expression, including TNF-α [16,17], IL-1β [14,16], MCP-1 [18-20] and bFGF [14,15,21,22] in the human vitreous samples with RD. Interestingly, hepatocyte growth factor (HGF) [33], TGF-β2 [14], platelet-derived growth factor (PDGF) [21], and vascular endothelial growth factor (VEGF) [34] are upregulated in the eyes of RD patients complicated with PVR but not in those with RD alone. The expression of HGF, TGF-β2, PDGF and VEGF did not change in this study (Figure 1). This is also in line with the fact that no PVR response is observed in the rat experimental RD model. Hence, the correlation between the findings in human patients and the data obtained in our animal model suggests that the experimental model of RD is well suited for studying the expression and functions of cytokines in RD-associated injury and photoreceptor cell degeneration.

Brain-derived neurotrophic factor [31], bFGF [31] and glia-derived neurotrophic factor [35] are known to be potent neuroprotective factors that can prevent photoreceptor degeneration induced by RD. Our results and a previous report [36] indicate that RD induces the expression of bFGF in a rat experimental RD. Interestingly, we found that the induction of bFGF was initiated at 24 h after RD, suggesting that this may be a secondary, self-protective response of photoreceptors towards injury. However, it should be noted that bFGF also induces a reactive gliosis in the retina, as demonstrated by the increase of GFAP expression in Müller cells [9-11,37]. In our model, we also detect GFAP expression at 24 h after RD (data not shown). Clinically, retinal gliosis worsens the visual prognosis of patients with RD [11], however the direct relation between retinal gliosis and photoreceptor degeneration remains unclear. Further studies will be necessary to clarify the etiology of the retinal gliosis and to determine whether retinal gliosis affects the viability of photoreceptors following RD.

Our time course studies show that TNF-α, IL-1β, and MCP-1 increase within 1 h after RD, suggesting that TNF-α, IL-1β, and MCP-1 are immediate pro-inflammatory responses following RD. TNF-α and IL-1β have been well documented to play a role in CNS pathologies [38,39] and work as pro-inflammatory factors to induce the expression of other cytokines and chemokines including MCP-1 [40,41]. In the RD model used here, TNF-α and IL-1β may increase the immediate inflammatory response following RD and influence the prolonged expression of MCP-1 and the subsequent retinal response including Müller cell hypertrophy [17], microglial cell activation [42] and monocyte recruitment [43].

The source of cytokines in the vitreous of retinal detached patients without PVR remains unknown, although it has been reported that cells invading the vitreous contribute critically as a source of cytokines in patients with PVR [44]. In this study, we show that astrocytes and Müller cells, in addition to the monocytes that invaded the subretinal space, are a major source of important cytokines and chemokines after RD. These results suggest that glial cells and monocytes play an important role in the pathogenesis of RD. An intervention aimed to control these activated cells may have a potential role in the treatment of RD.

A main finding of our study is the increased expression of MCP-1 in Müller cells after RD and that exogenous MCP-

1 increases the number of TUNEL-positive photoreceptors in the detached retina. MCP-1 expression in the CNS is generally low, however it increases after CNS injury, which results in activation, chemoattraction and infiltration of immune cells such as monocytes into the CNS [45-47]. In the model of experimental RD in the rat, microglial cell activation and macrophage recruitment into the subretinal space have been shown [32,42]. One of the major functions of subretinal macrophages is to phagocytose the apoptotic photoreceptors following RD [32], however the property of activated microglia and macrophages, which may lead to photoreceptor degeneration, remains uninvestigated. This may occur through MCP-1 binding to the CCR2 receptor, a seven transmembrane G protein-coupled receptor [48]. Initially, CCR2 was known to be expressed on immune cells, such as macrophages and activated lymphocytes [49,50]. However, growing evidence suggests that neurons [51], glial cells [51], and endothelium in the CNS [52,53] also express CCR2 and that it is upregulated under pathological conditions [47]. MCP-1 modulates calcium dynamics through CCR2 in cultured neurons [54,55]. In cultured photoreceptors, a calcium ionophore increases intracellular calcium levels, which results in photoreceptor death [56]. Taken together, the cytotoxic effect of MCP-1 on detached photoreceptors may be involved dual pathways, directly through CCR2 on photoreceptors or indirectly via macrophage/microglial cell activation.

In conclusion, we demonstrate that 4 proteins, TNF-α, IL-1β, MCP-1, and bFGF, are increased in the eye following experimental RD. TNF-α, IL-1β, and MCP-1 were detected very early after RD, while bFGF began to increase at 24 h. Retinal Müller cells and astrocytes are a major source of MCP-1 and IL-1 production, respectively, while bFGF and TNF-α are broadly distributed in the neural retina after RD. Exogenous MCP-1 independently induced RD-associated photoreceptor cell degeneration. Clarification of the function of these factors and the regulation of their expression may open new therapeutic avenues to treat RD and prevent vision loss in human patients.

ACKNOWLEDGEMENTS

The authors thank Charles Vanderburg, PhD for help and instruction in the LCM study and Tara A. Young, MD (Jules Stein Eye Institute, David Geffen School of Medicine at UCLA) for discussion.

REFERENCES

1. Chang CJ, Lai WW, Edward DP, Tso MO. Apoptotic photoreceptor cell death after traumatic retinal detachment in humans. Arch Ophthalmol 1995; 113:880-6.
2. Cook B, Lewis GP, Fisher SK, Adler R. Apoptotic photoreceptor degeneration in experimental retinal detachment. Invest Ophthalmol Vis Sci 1995; 36:990-6.
3. Luthert PJ, Chong NH. Photoreceptor rescue. Eye 1998; 12:591-6.
4. Arroyo JG, Yang L, Bula D, Chen DF. Photoreceptor apoptosis in human retinal detachment. Am J Ophthalmol 2005; 139:605-10.
5. Zacks DN, Hanninen V, Pantcheva M, Ezra E, Grosskreutz C, Miller JW. Caspase activation in an experimental model of retinal detachment. Invest Ophthalmol Vis Sci 2003; 44:1262-7.
6. Zacks DN, Zheng QD, Han Y, Bakhru R, Miller JW. FAS-mediated apoptosis and its relation to intrinsic pathway activation in an experimental model of retinal detachment. Invest Ophthalmol Vis Sci 2004; 45:4563-9.
7. Limb GA, Hollifield RD, Webster L, Charteris DG, Chignell AH. Soluble TNF receptors in vitreoretinal proliferative disease. Invest Ophthalmol Vis Sci 2001; 42:1586-91.
8. Cardone MH, Roy N, Stennicke HR, Salvesen GS, Franke TF, Stanbridge E, Frisch S, Reed JC. Regulation of cell death protease caspase-9 by phosphorylation. Science 1998; 282:1318-21.
9. Geller SF, Lewis GP, Fisher SK. FGFR1, signaling, and AP-1 expression after retinal detachment: reactive Muller and RPE cells. Invest Ophthalmol Vis Sci 2001; 42:1363-9.
10. Lewis GP, Fisher SK. Up-regulation of glial fibrillary acidic protein in response to retinal injury: its potential role in glial remodeling and a comparison to vimentin expression. Int Rev Cytol 2003; 230:263-90.
11. Sethi CS, Lewis GP, Fisher SK, Leitner WP, Mann DL, Luthert PJ, Charteris DG. Glial remodeling and neural plasticity in human retinal detachment with proliferative vitreoretinopathy. Invest Ophthalmol Vis Sci 2005; 46:329-42.
12. Nagasaki H, Shinagawa K, Mochizuki M. Risk factors for proliferative vitreoretinopathy. Prog Retin Eye Res 1998; 17:77-98.
13. Tseng W, Cortez RT, Ramirez G, Stinnett S, Jaffe GJ. Prevalence and risk factors for proliferative vitreoretinopathy in eyes with rhegmatogenous retinal detachment but no previous vitreoretinal surgery. Am J Ophthalmol 2004; 137:1105-15.
14. Kon CH, Occleston NL, Aylward GW, Khaw PT. Expression of vitreous cytokines in proliferative vitreoretinopathy: a prospective study. Invest Ophthalmol Vis Sci 1999; 40:705-12.
15. La Heij EC, van de Waarenburg MP, Blaauwgeers HG, Kessels AG, Liem AT, Theunissen C, Steinbusch H, Hendrikse F. Basic fibroblast growth factor, glutamine synthetase, and interleukin-6 in vitreous fluid from eyes with retinal detachment complicated by proliferative vitreoretinopathy. Am J Ophthalmol 2002; 134:367-75.
16. El-Ghrably IA, Dua HS, Orr GM, Fischer D, Tighe PJ. Detection of cytokine mRNA production in infiltrating cells in proliferative vitreoretinopathy using reverse transcription polymerase chain reaction. Br J Ophthalmol 1999; 83:1296-9.
17. Limb GA, Daniels JT, Pleass R, Charteris DG, Luthert PJ, Khaw PT. Differential expression of matrix metalloproteinases 2 and 9 by glial Muller cells: response to soluble and extracellular matrix-bound tumor necrosis factor-alpha. Am J Pathol 2002; 160:1847-55.
18. Abu el-Asrar AM, Van Damme J, Put W, Veckeneer M, Dralands L, Billiau A, Missotten L. Monocyte chemotactic protein-1 in proliferative vitreoretinal disorders. Am J Ophthalmol 1997; 123:599-606.
19. Capeans C, De Rojas MV, Lojo S, Salorio MS. C-C chemokines in the vitreous of patients with proliferative vitreoretinopathy and proliferative diabetic retinopathy. Retina 1998; 18:546-50.
20. Mitamura Y, Takeuchi S, Yamamoto S, Yamamoto T, Tsukahara I, Matsuda A, Tagawa Y, Mizue Y, Nishihira J. Monocyte chemotactic protein-1 levels in the vitreous of patients with proliferative vitreoretinopathy. Jpn J Ophthalmol 2002; 46:218-21.
21. Cassidy L, Barry P, Shaw C, Duffy J, Kennedy S. Platelet derived growth factor and fibroblast growth factor basic levels in the vitreous of patients with vitreoretinal disorders. Br J Ophthalmol 1998; 82:181-5.

22. La Heij EC, Van De Waarenburg MP, Blaauwgeers HG, Kessels AG, De Vente J, Liem AT, Steinbusch H, Hendrikse F. Levels of basic fibroblast growth factor, glutamine synthetase, and interleukin-6 in subretinal fluid from patients with retinal detachment. Am J Ophthalmol 2001; 132:544-50.
23. Nakazawa T, Morii H, Tamai M, Mori N. Selective upregulation of RB3/stathmin4 by ciliary neurotrophic factor following optic nerve axotomy. Brain Res 2005; 1061:97-106.
24. Livak KJ, Schmittgen TD. Analysis of relative gene expression data using real-time quantitative PCR and the 2(-Delta Delta C(T)) Method. Methods 2001; 25:402-8.
25. Sgroi DC, Teng S, Robinson G, LeVangie R, Hudson JR Jr, Elkahloun AG. In vivo gene expression profile analysis of human breast cancer progression. Cancer Res 1999; 59:5656-61.
26. Huang W, Dobberfuhl A, Filippopoulos T, Ingelsson M, Fileta JB, Poulin NR, Grosskreutz CL. Transcriptional up-regulation and activation of initiating caspases in experimental glaucoma. Am J Pathol 2005; 167:673-81.
27. Nakazawa T, Endo S, Shimura M, Kondo M, Ueno S, Tamai M. Retinal G-substrate, potential downstream component of NO/cGMP/PKG pathway, is located in subtype of retinal ganglion cells and amacrine cells with protein phosphatases. Brain Res Mol Brain Res 2005; 135:58-68.
28. Nakazawa T, Nakano I, Sato M, Nakamura T, Tamai M, Mori N. Comparative expression profiles of Trk receptors and Shc-related phosphotyrosine adapters during retinal development: potential roles of N-Shc/ShcC in brain-derived neurotrophic factor signal transduction and modulation. J Neurosci Res 2002; 68:668-80.
29. Nakazawa T, Shimura M, Tomita H, Akiyama H, Yoshioka Y, Kudou H, Tamai M. Intrinsic activation of PI3K/Akt signaling pathway and its neuroprotective effect against retinal injury. Curr Eye Res 2003; 26:55-63.
30. Nakazawa T, Tamai M, Mori N. Brain-derived neurotrophic factor prevents axotomized retinal ganglion cell death through MAPK and PI3K signaling pathways. Invest Ophthalmol Vis Sci 2002; 43:3319-26.
31. Hisatomi T, Sakamoto T, Goto Y, Yamanaka I, Oshima Y, Hata Y, Ishibashi T, Inomata H, Susin SA, Kroemer G. Critical role of photoreceptor apoptosis in functional damage after retinal detachment. Curr Eye Res 2002; 24:161-72.
32. Hisatomi T, Sakamoto T, Sonoda KH, Tsutsumi C, Qiao H, Enaida H, Yamanaka I, Kubota T, Ishibashi T, Kura S, Susin SA, Kroemer G. Clearance of apoptotic photoreceptors: elimination of apoptotic debris into the subretinal space and macrophage-mediated phagocytosis via phosphatidylserine receptor and integrin alphavbeta3. Am J Pathol 2003; 162:1869-79.
33. Mitamura Y, Takeuchi S, Matsuda A, Tagawa Y, Mizue Y, Nishihira J. Hepatocyte growth factor levels in the vitreous of patients with proliferative vitreoretinopathy. Am J Ophthalmol 2000; 129:678-80.
34. Ogata N, Nishikawa M, Nishimura T, Mitsuma Y, Matsumura M. Inverse levels of pigment epithelium-derived factor and vascular endothelial growth factor in the vitreous of eyes with rhegmatogenous retinal detachment and proliferative vitreoretinopathy. Am J Ophthalmol 2002; 133:851-2.
35. Wu WC, Lai CC, Chen SL, Xiao X, Chen TL, Tsai RJ, Kuo SW, Tsao YP. Gene therapy for detached retina by adeno-associated virus vector expressing glial cell line-derived neurotrophic factor. Invest Ophthalmol Vis Sci 2002; 43:3480-8.
36. Ozaki S, Radeke MJ, Anderson DH. Rapid upregulation of fibroblast growth factor receptor 1 (flg) by rat photoreceptor cells after injury. Invest Ophthalmol Vis Sci 2000; 41:568-79.
37. Fisher SK, Lewis GP. Muller cell and neuronal remodeling in retinal detachment and reattachment and their potential consequences for visual recovery: a review and reconsideration of recent data. Vision Res 2003; 43:887-97.
38. Merrill JE. Tumor necrosis factor alpha, interleukin 1 and related cytokines in brain development: normal and pathological. Dev Neurosci 1992; 14:1-10.
39. Yoshioka M, Bradley WG, Shapshak P, Nagano I, Stewart RV, Xin KQ, Srivastava AK, Nakamura S. Role of immune activation and cytokine expression in HIV-1-associated neurologic diseases. Adv Neuroimmunol 1995; 5:335-58.
40. Bian ZM, Elner SG, Yoshida A, Kunkel SL, Su J, Elner VM. Activation of p38, ERK1/2 and NIK pathways is required for IL-1beta and TNF-alpha-induced chemokine expression in human retinal pigment epithelial cells. Exp Eye Res 2001; 73:111-21.
41. Crane IJ, Wallace CA, McKillop-Smith S, Forrester JV. Control of chemokine production at the blood-retina barrier. Immunology 2000; 101:426-33.
42. Lewis GP, Sethi CS, Carter KM, Charteris DG, Fisher SK. Microglial cell activation following retinal detachment: a comparison between species. Mol Vis 2005; 11:491-500.
43. Bamforth SD, Lightman SL, Greenwood J. Ultrastructural analysis of interleukin-1 beta-induced leukocyte recruitment to the rat retina. Invest Ophthalmol Vis Sci 1997; 38:25-35.
44. El-Ghrably IA, Dua HS, Orr GM, Fischer D, Tighe PJ. Intravitreal invading cells contribute to vitreal cytokine milieu in proliferative vitreoretinopathy. Br J Ophthalmol 2001; 85:461-70.
45. Babcock AA, Kuziel WA, Rivest S, Owens T. Chemokine expression by glial cells directs leukocytes to sites of axonal injury in the CNS. J Neurosci 2003; 23:7922-30.
46. Lahrtz F, Piali L, Spanaus KS, Seebach J, Fontana A. Chemokines and chemotaxis of leukocytes in infectious meningitis. J Neuroimmunol 1998; 85:33-43.
47. Xia MQ, Hyman BT. Chemokines/chemokine receptors in the central nervous system and Alzheimer's disease. J Neurovirol 1999; 5:32-41.
48. Dzenko KA, Andjelkovic AV, Kuziel WA, Pachter JS. The chemokine receptor CCR2 mediates the binding and internalization of monocyte chemoattractant protein-1 along brain microvessels. J Neurosci 2001; 21:9214-23.
49. Huffnagle GB, Traynor TR, McDonald RA, Olszewski MA, Lindell DM, Herring AC, Toews GB. Leukocyte recruitment during pulmonary Cryptococcus neoformans infection. Immunopharmacology 2000; 48:231-6.
50. Reape TJ, Groot PH. Chemokines and atherosclerosis. Atherosclerosis 1999; 147:213-25.
51. Banisadr G, Queraud-Lesaux F, Boutterin MC, Pelaprat D, Zalc B, Rostene W, Haour F, Parsadaniantz SM. Distribution, cellular localization and functional role of CCR2 chemokine receptors in adult rat brain. J Neurochem 2002; 81:257-69.
52. Stamatovic SM, Keep RF, Kunkel SL, Andjelkovic AV. Potential role of MCP-1 in endothelial cell tight junction 'opening': signaling via Rho and Rho kinase. J Cell Sci 2003; 116:4615-28.
53. Stamatovic SM, Shakui P, Keep RF, Moore BB, Kunkel SL, Van Rooijen N, Andjelkovic AV. Monocyte chemoattractant protein-1 regulation of blood-brain barrier permeability. J Cereb Blood Flow Metab 2005; 25:593-606.
54. Banisadr G, Gosselin RD, Mechighel P, Kitabgi P, Rostene W, Parsadaniantz SM. Highly regionalized neuronal expression of monocyte chemoattractant protein-1 (MCP-1/CCL2) in rat brain: Evidence for its colocalization with neurotransmitters and neuropeptides. J Comp Neurol 2005; 489:275-92.

55. van Gassen KL, Netzeband JG, de Graan PN, Gruol DL. The chemokine CCL2 modulates Ca2+ dynamics and electrophysiological properties of cultured cerebellar Purkinje neurons. Eur J Neurosci 2005; 21:2949-57.

56. Sharma AK, Rohrer B. Calcium-induced calpain mediates apoptosis via caspase-3 in a mouse photoreceptor cell line. J Biol Chem 2004; 279:35564-72.

The print version of this article was created on 7 Aug 2006. This reflects all typographical corrections and errata to the article through that date. Details of any changes may be found in the online version of the article. α